Molecular-dynamics-based analysis of the absorption spectra of Nd³⁺-doped Na⁺ β″-alumina

Mats Wolf, Sverker Edvardsson, Miguel A. Zendejas, and John O. Thomas

Institute of Chemistry, University of Uppsala, Box 531, S-751 21 Uppsala, Sweden

(Received 27 April 1993)

The polarized absorption spectra of Nd³⁺-doped Na⁺ β″-alumina have been treated theoretically for five neodymium concentrations. The perturbing crystal field, needed in the Judd-Ofelt analysis, is calculated from a molecular-dynamics simulation for each composition. Oscillator strengths and Judd-Ofelt intensity parameters are calculated using a point-charge model at each time step in the simulation for each of the Nd³⁺ ions in the simulation box. A study of the effect of the dynamics of the system on these parameters was also made. The theoretical results thus obtained are compared to experiment. It is shown that the absorption spectra can be explained essentially on the basis of the special structural situation of the Nd³⁺ ions in these materials.

I. INTRODUCTION

Sodium β″-alumina is a solid electrolyte with a unique ability to undergo ion exchange. The structure consists of close-packed spinel-like blocks, and more open, disordered *conduction planes*. It is into these that the exchange can take place. The material has been studied primarily for its liquid-like, almost two-dimensional (2D) transport of ions within these planes; but the possibility to incorporate transition-metal and lanthanide ions also has led to investigations of the optical properties of the ion-exchanged β″-aluminas. Na⁺ β″-alumina doped with trivalent rare-earth (RE) ions have been shown to possess quite unusual optical properties, which can find application in the areas of solid-state lasers and other optoelectronic devices. Attention has earlier been focused mainly on Nd³⁺-doped systems, but Er³⁺-doped Na⁺ β″-alumina has also been studied.[1]

Laser action was first demonstrated in Nd³⁺-doped Na⁺ β″-alumina by Jansen et al.,[2] and the absorption spectra revealed an anomalously high oscillator strength for the *hypersensitive* transition, $^4I_{9/2} \rightarrow {}^4G_{5/2}$.[3] The standard method for analyzing rare-earth transition intensities is based upon the Judd-Ofelt (JO) theory[4,5] in which, typically, three phenomenological parameters (Ω_λ) are fitted to experimental data. These parameters can then be used for comparing oscillator strengths and predicting emission cross sections in different laser materials. In principle, it is also possible to determine the oscillator strengths (and Ω_λ:s) *a priori* by calculating the ligand crystal field at the RE site. The field is introduced into the theory as a first-order perturbation, responsible for the mixing in of opposite parity wave functions into the 4f states between which the electric-dipole transitions occur. Earlier attempts to calculate theoretical Ω parameters using the original formulation have been more or less successful,[3,4,6,7] and refinements to the theory have been proposed (see, for example, Refs. 3 and 8, and references therein).

In two previous studies of the absorption spectra of Nd³⁺-doped Na⁺ β″-alumina, theoretical JO analyses were made to explain the experimental spectra. A model was used for the crystal-field calculation which included nearest-neighbor atoms only.[3,7] Both attempts met with little success, however. Different explanations were given for the discrepancy between experimental and theoretical JO parameters. The main deficiencies in both studies are (i) Too little of the local environment is included for the crystal-field calculations; and (ii) The unusual disordered structural situation involving the rare-earth ions in these materials is inadequately treated. The two are clearly related. The disorder in the conduction plane leads to a large number of possible environments for the Nd³⁺ ions. One way to treat this problem is to use the technique proposed by Edvardsson, Wolf, and Thomas,[9] where the JO theory is combined with molecular-dynamics (MD) simulation to determine the environments of the RE ions. The positions of the surrounding ions are, at each time step in the simulation, used to calculate the instantaneous crystal field and subsequently the JO parameters and oscillator strengths. This makes it possible to investigate how ions in different structural situations contribute to the absorption spectrum and how the various transitions are affected by fluctuations in the local environment, and particularly by the dynamics of the conduction planes. In the current work, this technique has been applied to five differently doped Nd³⁺-doped Na⁺ β″-aluminas, where the crystal-field calculations have been made using a point-charge model. The theoretical results are compared to experimental values to obtain greater insight into the structure/property relationships in these types of material.

II. THE STRUCTURE OF Nd³⁺-DOPED Na⁺ β″-ALUMINA

The nonstoichiometric compound sodium β″-alumina (nominally $Na_{1+x}Mg_xAl_{11-x}O_{17}$, with $x = \frac{2}{3}$) is a solid electrolyte in which the Na⁺ ions can be ion exchanged at relatively low temperatures ($\sim$ 500–900 K) for a wide variety of mono-, di- , and trivalent ions as well as some molecular-ion species (see Ref. 10, and references quoted therein). This property is a result of the structure of Na⁺ β″alumina, which consists of close-packed *spinel blocks* comprising Al³⁺, Mg,²⁺, and O²⁻ ions, and more open, liquidlike regions (*conduction planes*), in which the

mobile Na^+ ions are situated in the hexagonal pathways around a single supporting oxygen ion [O(5) or *column oxygen*]. This atom forms the link between adjacent spinel blocks through Al-O-Al bonds. The space group for the crystalline framework (spinel blocks and column oxygen) is $R\bar{3}m$, with hexagonal axes $a=b=5.614$ Å and $c=33.85$ Å. Schematic illustrations of the structure and the conduction plane are given in Fig. 1. Two possible sites for the cations are indicated in

(a)

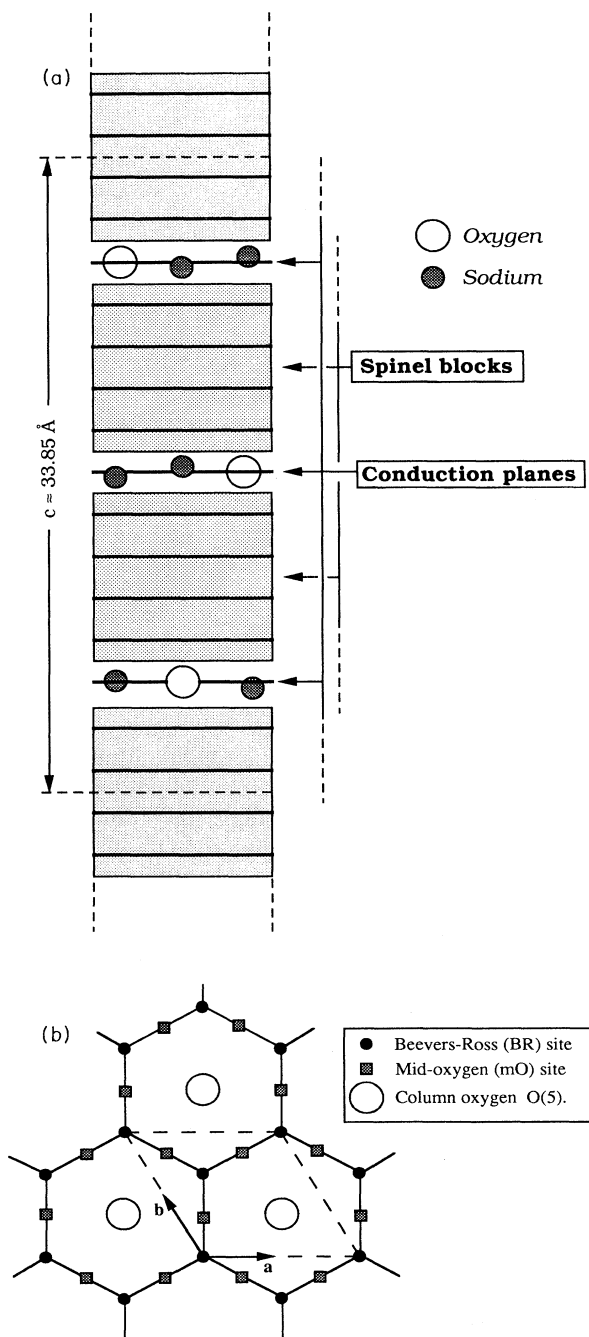c ≈ 33.85 Å

○ Oxygen
● Sodium

Spinel blocks

Conduction planes

(b)

● Beevers-Ross (BR) site
▨ Mid-oxygen (mO) site
◯ Column oxygen O(5).

FIG. 1. Schematic block structure of Na^+ β''-alumina (a), and the 2D conduction planes (b).

Fig. 1(b): the seven-coordinated *Beevers-Ross* (BR) site and the eight-coordinated midoxygen (mO) site with C_{3v} and C_{2h} symmetry, respectively. In $Na^+\beta''$-alumina, sodium ions occupy, on average, five out of six BR sites. While this nonstoichiometry is essential to the ion-exchange and ion-transport properties, it makes it difficult to define a local structure on the basis of the space- and time-averaged picture of the ionic distribution obtained by diffraction. It is this local structure which is needed to calculate, for example, the Stark field. It is clear that the effective point symmetries within the conduction plane, as defined by the spinel-block and column-oxygen atoms, is broken by the mobile ions in the conduction layer.

X-ray-diffraction studies have so far been made of two differently Nd^{3+}-doped Na^+ β''-aluminas: 100% (Ref. 11) and 64% (Ref. 12). In the fully exchanged sample, 95% of the Nd^{3+} ions were found at mO sites and the rest at BR sites; in the mixed-ion system, the neodymium ions were distributed between the BR and mO sites roughly in the ratio 1:2. Electron-spin resonance (ESR) and optical-absorption spectroscopy have further shown that Nd^{3+} ions behave quite differently depending upon the degree of exchange. In a sample with low Nd^{3+} concentration (18%), the exchanged RE ions were observed only as isolated species while, in a fully exchanged sample, there were indications that Nd^{3+} ions occurred both as isolated species and as discrete pairs.[13]

III. JUDD-OFELT THEORY

The Judd-Ofelt[4,5] theory was developed to explain the observed intensities in optical-absorption spectra for RE ions. Radiative transitions between $4f^N$ states within these ions are found to be predominantly electric-dipole in nature; the theory takes into account the mixing of $4f^{N-1}5d$ and $4f^{N-1}5g$ states with the $4f^N$ states by the odd-parity terms static crystal-field expansion. This mixing renders these otherwise parity-forbidden transitions allowed. For this work, a slightly modified theory has been used which takes account of polarization dependence in biaxial and anisotropic uniaxial crystals, thus making it possible to analyze polarized spectra,[3] i.e., averaging is not made over all directions [Eq. (15) in Ref. 4]. All formulas relating to the present work and a more detailed description of the theory can be found in Ref. 9. Only the essentials are summarized here.

The easiest way to calculate the crystal-field parameters (CFP) in an atomic compound is to consider the environmental ions as consisting of point charges. The expression for the CFP's can then be written

$$A_{t,p}=(-1)^p\left[\frac{4\pi}{2t+1}\right]^{1/2}\sum_j g_j e^2 R_j^{-(t+1)}Y_{t,-p}(\Theta_j,\Phi_j) \ ,$$

(1)

where the sum runs over all point charges $(-ge)$ located at positions (R,Θ,Φ), where the spherical coordinate system has its origin at the RE site. These parameters are then included in the expression for the oscillator strength via the Ω parameters:

$$P_q = \chi \frac{8\pi^2 m \nu}{(2J+1)} \sum_{h\lambda=2,4,6} \Omega_{\lambda,q} |\langle 4f^n[L,S]J\|U^{(\lambda)}\|f^n[L',S']J'\rangle|^2 , \qquad (2)$$

in which

$$\Omega_{\lambda,q} = \sum_{t,\tau,p} (2\lambda+1) A_{t,p}^* A_{\tau,p} \Xi(t,\lambda)\Xi(\tau,\lambda) \begin{bmatrix} 1 & \lambda & t \\ q & -p-q & p \end{bmatrix} \begin{bmatrix} 1 & \lambda & \tau \\ q & -p-q & p \end{bmatrix} , \qquad (3)$$

where $t = 1,3,5,7$; $\tau = 1,3,\ldots,t$; $p = -\tau, -\tau+1, \ldots, \tau$, and

$$\Xi(t,\lambda) = 2 \sum (2l+1)(2l'+1)(-1)^{l+l'} \begin{Bmatrix} 1 & \lambda & t \\ l & l' & l \end{Bmatrix} \begin{bmatrix} l & 1 & l' \\ 0 & 0 & 0 \end{bmatrix} \begin{bmatrix} l' & t & l \\ 0 & 0 & 0 \end{bmatrix} \frac{\langle nl|r|n'l'\rangle\langle nl|r^t|n'l'\rangle}{\Delta E(n'l')} , \qquad (4)$$

where the sum runs over values of n' and l' of the excited configurations.

The q is introduced to take account for the polarization dependence: $q=0$ corresponds to π polarization ($E\|c$) and $q=\pm1$ to σ polarization ($E\perp c$). The $U^{(\lambda)}$ are the doubly reduced matrix elements between the initial and final manifold, $\langle nl|r|n'l'\rangle$ are the interconfiguration radial integrals, and $\Delta E(n'l')$ are the energy separations between the ground configuration $(4f^N)$ and the excited configurations $[4f^{N-1}(n'l')]$.

IV. MOLECULAR-DYNAMICS SIMULATION

The molecular-dynamics (MD) simulation technique has been used for several β''- and β-aluminas to obtain a better understanding of the conduction mechanisms within these materials (see, for example, Refs. 14 and 15). The method treats the system as a classical ensemble of particles (ions), and the interactions between the particles are expressed through potential functions. In this work these were assumed to be of the Born-Mayer-Huggins form [Eq. (10) in Ref. 9], where the velocities and positions of the particles are obtained by simultaneously solving Newton's equation of motion for each particle in the *simulation box*. The technique makes it possible to study individual ions, and also provides local order not obtainable from conventional diffraction studies of the β''- and β-aluminas. The principles of the method are given in Ref. 9, and will not be repeated here; only specific details relating to the present system will be referred to.

A $6a \times 6b \times 1c$ simulation box was used in which the initial positional parameters for the ions were taken from diffraction study, and the values for the parameters A, ρ, and C in the potential function where taken from the

literature,[16,17] with the exception of the Nd^{3+}-Na^+ potential, which was assumed to be of the same form as the Al^{3+}-Na^+ potential; and the Nd^{3+}-Nd^{3+} interaction, for which a Coulomb term only was used. The assumption was made that the material is totally ionic, i.e., the charges on the Nd, Al, Mg, Na, and O where taken to be $+3$, $+3$, $+2$, $+1$, and -2, respectively. MD simulation were made for five different compositions: 20, 30, 40, 60, and 100 % Nd^{3+} exchange. The number of cations in one of the conduction planes, as well as the total number of ions in the simulation box is given in Table I. To ensure that the ions in the conduction planes move freely and independently of their initial configuration, the simulation was started with a "heat treatment," i.e., each system was initialized and equilibrated at a high temperature (1000 K) for a minimum of 4000 time steps, each of 2.0 fs. The temperature was then lowered in two steps, each of at least 2000 time steps, to the final value of 300 K. After this treatment, the ionic positions could be stored for the subsequent analysis.

Comparing results from the MD simulations to crystallographic results (64 and 100 % exchange), it was found that the ionic distribution in the conduction plane agreed quite satisfactory. A rough comparison is made in Table II (for 500 time steps) of the Nd^{3+} distribution over BR and mO sites in one of the conduction planes. The Na^+ ions only occupy BR sites. Occasionally however, they will pass through mO sites when diffusing from one BR site to another. The trajectories for 4000 time steps in the fully exchanged composition at 300 K are shown in Figs. 2(a) and 2(b) both as a section through the simulation box in the conduction plane, and superposed into one cell for comparison with the crystallographic result [Fig. 2(c)].

TABLE I. Numbers of Na^+ and Nd^{3+} cations in the conduction plane and the total number of ions in the simulation box for the different Nd^{3+}-doped Na^+ β''-alumina compositions.

% (Nd^{3+})	No. of Na^+ ions	No. of Nd^{3+} ions	Total No.
20	48	4	3180
30	42	6	3168
40	36	8	3156
60	24	12	3132
100	0	20	3084

TABLE II. Nd^{3+} site occupations (in %) in BR and mO sites obtained from MD simulation and crystallography (Refs. 11 and 12).

% (Nd^{3+})		BR	mO
60	MD	43	57
64	Cryst.	35	65
100	MD	5	95
100	Cryst.	5	95

V. ANALYSIS AND DISCUSSION

A. Method of calculation

It is necessary that the number of Nd^{3+} ions in the simulation box should be as large as possible to properly represent the large number of different structural situations for the Nd^{3+} ions. The ions chosen for the analysis were taken from one of the conduction planes of the simulation box (see Table I). It is clear, however, that the
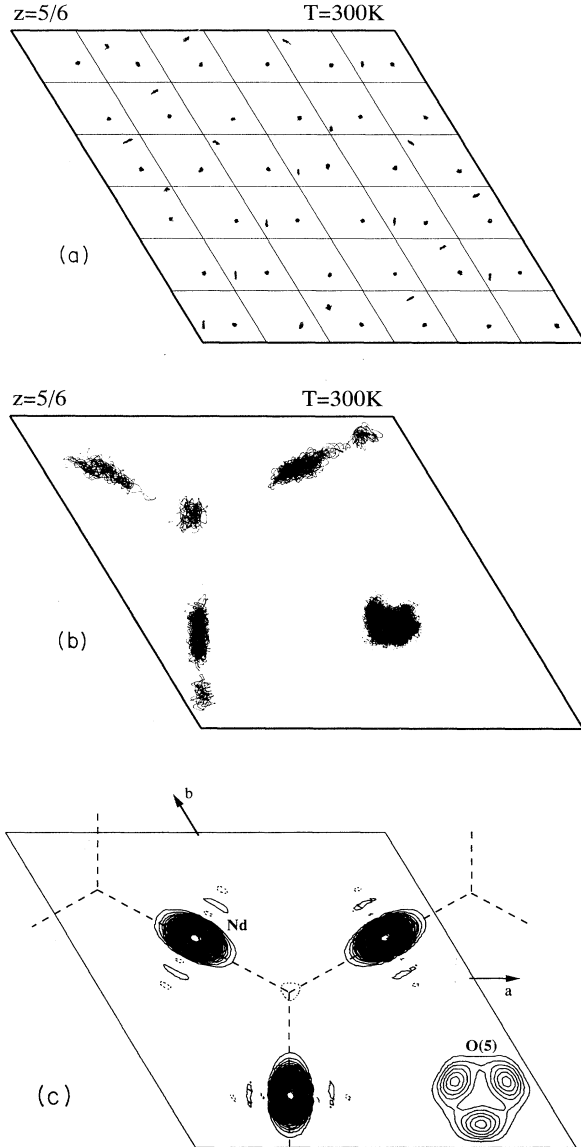

(a)

(b)

(c)

FIG. 2. Trajectories of the ions in the conduction plane obtained from 4000 MD time steps at a target temperature of 300 K for the 100% composition: (a) The projected $6a \times 6a \times 1c$ simulation, (b) A superposition into the crystallographic unit cell, (c) The crystallographically determined ion distribution (Ref. 11).

limited number of discrete neodymium ions in a $6 \times 6 \times 1$ simulations box will be insufficient to represent all possible types of Nd^{3+} environment, especially at low concentrations.

The same set of $U^{(\lambda)}$, radial integrals, and energy denominators were used, to facilitate comparison with results from the two previous *a priori* calculations for these materials.[3,7] However, the values for the radial integrals taken from Ref. 4 are interpolated from calculations for Pr^{3+} and Tm^{3+}, and the energy denominators from experimental values of Yb^{3+} and Ce^{3+}. The radial integrals have therefore been recalculated here (see Sec. V F) using the Hartree-Fock-Dirac method with Slater-type orbitals. Furthermore, the value for the energy denominator $\Delta E(5d)$ [see Eq. (4)] was the one given in Ref. 18. See Table III. The $\langle nl|r^u|n'l'\rangle$ integrals for u even are included, since the approximation is made that

$$\sum_{n'} \langle nl|r|n'l'\rangle \langle nl|r^t|n'l'\rangle = \langle nl|r^{t+1}|n'l'\rangle$$

for $l'=g$.[4]

The positions for all ions in the simulation box were stored for 500 time steps. The Nd^{3+} ions from the $z=\frac{1}{2}$ or $\frac{5}{6}$ conduction planes were extracted at each time step, and with them (for each Nd^{3+} ion) all surrounding ions within a radius of 12 Å. These constituted the calculation spheres used for the calculation of the crystal field for each Nd^{3+} ion [Eq. (1)]. The $A_{t,p}$ parameters [Eq. (1)] and subsequently the $\Omega_{\lambda,q}$ and P_q parameters [Eqs. (2) and (3)] were evaluated at each time step. This calculation was facilitated by reproducing the original $6 \times 6 \times 1$ simulation box in the a, b, and c directions in such a way as to create an $18a \times 18b \times 2c$ cell. The calculation could then be performed for the ions in the central box. The 12-Å radius for the calculation sphere was the result of a practical limit set by our present computer capacity. Ideally, a larger radius should be used to calculate the Ω_2 parameter, since Ω_λ is determined by the $A_{t,p}$ parameters with $t=\lambda-1$ and $\lambda+1$, and these vary as $R^{-(t+1)}$ [see Eq. (1)]. Values of Ω_6 and Ω_4 should thus converge within a 12-Å sphere, while the R^{-2} dependence of $A_{1,p}$ may result in a very slow convergence for Ω_2 for increasing radius. This will depend, however, on the site sym-

TABLE III. Values of radial integrals and energy denominators (in atomic units).

Integral	Ref. 4	This work
$\langle 4f|r|5d\rangle$	0.87	0.83
$\langle 4f|r^3|5d\rangle$	5.17	4.45
$\langle 4f|r^5|5d\rangle$	47.1	37.3
$\langle 4f|r^2|4f\rangle$	1.39	1.22
$\langle 4f|r^4|4f\rangle$	4.96	3.87
$\langle 4f|r^6|4f\rangle$	36.4	26.1
$\langle 4f|r^8|4f\rangle$	450	307
$\Delta(5d)$	0.26	0.32[a]
$\Delta(n'g)$	0.76	$\leftarrow$

[a]Reference 18.

metry ($A_{1,p}$ may be zero), and on the type of material. The effect of using different calculation spheres is displayed for the 30% Nd^{3+} composition in Fig. 3. A 12-Å radius essentially reproduces the crystal field obtained for an "infinite" radius, since this value includes nearest-neighbor conduction planes (11 Å away). Increasing R to 13 Å results in the inclusion of some of the next layers of O^{2-} ions. This brings about the increase of the Ω_2 parameter seen in Fig. 3(a). Alternative approaches would be (i) to create a spherical environment comprising a set of adjacent unit cells;[9] or (ii) to use an Ewald summation.[19] Both alternatives demand a computational capability beyond our current resources.
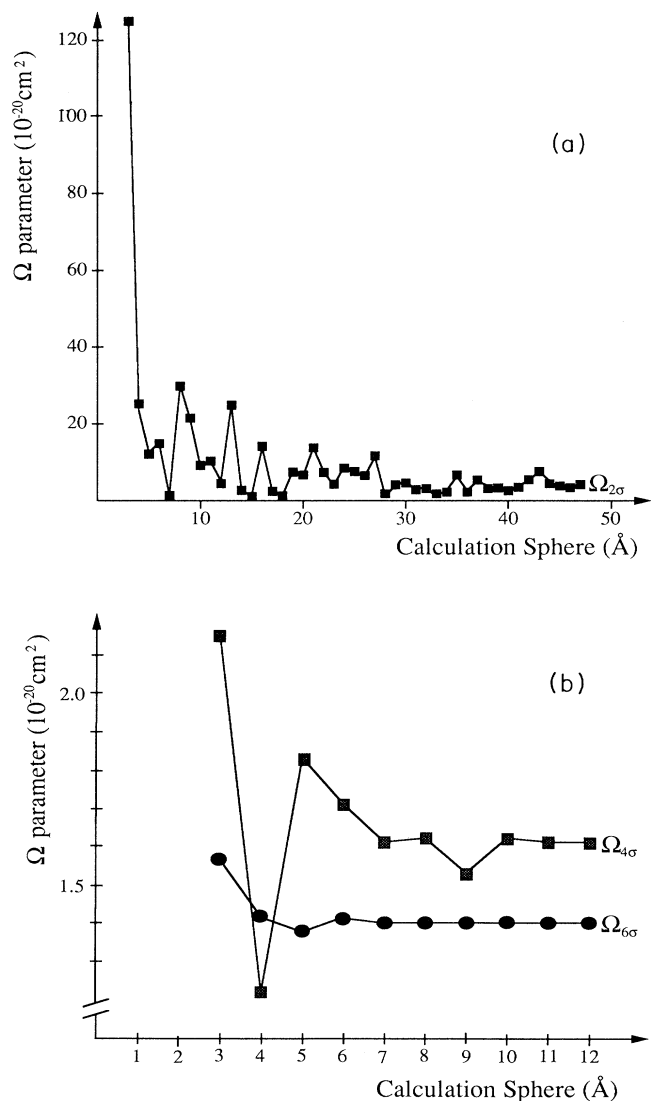

FIG. 3. The variation of $\Omega_{\lambda,\sigma}$ parameters calculated for different calculation-sphere radii, for one particular ion at a given time step for the 30% composition: (a) $\Omega_{2,\sigma}$, (b) $\Omega_{4,\sigma}$, and $\Omega_{6,\sigma}$.

B. Previous studies

Accurate experimental studies have been performed for samples with approximately 27.5% (Ref. 3) and 38.5% (Ref. 7) of the Na^+ ions exchanged for Nd^{3+} ions. In the study made by Alfrey et al.,[3] other concentrations were reported, but the results were only presented graphically. In a more recent study,[7] both π- and σ-polarized spectra were obtained, while only σ-polarized spectra were obtained in Ref. 3. In both studies, it is emphasized that π-polarized spectra are more difficult to handle experimentally, partly because of the shape of the crystals: They are usually several millimeters in the a and b directions but only a fraction of a millimeter in the c direction; and also since light propagated in a direction perpendicular to the c axis is essentially waveguided through the crystal by the 2D conduction plane; this tends to scramble the polarization of the incident light, resulting in randomly polarized data. We therefore focus here mainly on the σ-polarized case. In both these studies, a priori calculations of the Ω parameters were made for the Nd^{3+}-doped β''-alumina to explain the absorption spectra. In one study,[3] only the nearest-neighbor oxygens were included in the calculation of the crystal field. Their coordinates were then treated as independently adjustable parameters to study how these affected the resulting values. Unfortunately, although the applied distortions gave a reasonable agreement, they were not consistent with crystallographic observations.[11] It was nevertheless concluded that displacements of the Nd^{3+} and O^{2-} ions from their mean positions were essential to a complete understanding of the absorption spectra. Dai and Stafsudd[7] included nearest-neighbor oxygens, but used both mO and BR sites for the Nd^{3+} ions. An additional term to take account of ligand polarizability was also included in the expression for the $A_{t,p}$ parameters. This resulted in fair agreement for the Ω_2 and Ω_6 parameters for the mO site, and the Ω_2 parameter for the BR site, while the Ω_4 and Ω_6 parameters for the BR site were roughly an order of magnitude smaller than the experimental JO parameters. They suggested that this was due to neglect of the shielding effect, and exclusion of contributions from the $4f$ wavefunction expansion in the lattice. No investigation was made of the explicit effect on the numerical values obtained.

C. Oscillator strengths and JO parameters

Figure 4 plots the JO intensity parameters for Nd^{3+} ion site for various concentrations. The experimental values taken from Refs. 3 and 7, and the average theoretical values taken over all sites and MD steps are also included. The average values are also given in Table IV, while Fig. 5 shows the calculated oscillator strengths (averaged over all MD steps and sites) for the 30% composition, compared to the experimental values for the 27.5% exchanged sample. In making comparison with experimental results,[7] the wavelengths given are generally a superposition of a number of unresolved transitions.

We see that individual ions acquire a wide range of Ω_λ parameters. This suggests that the number of ions used
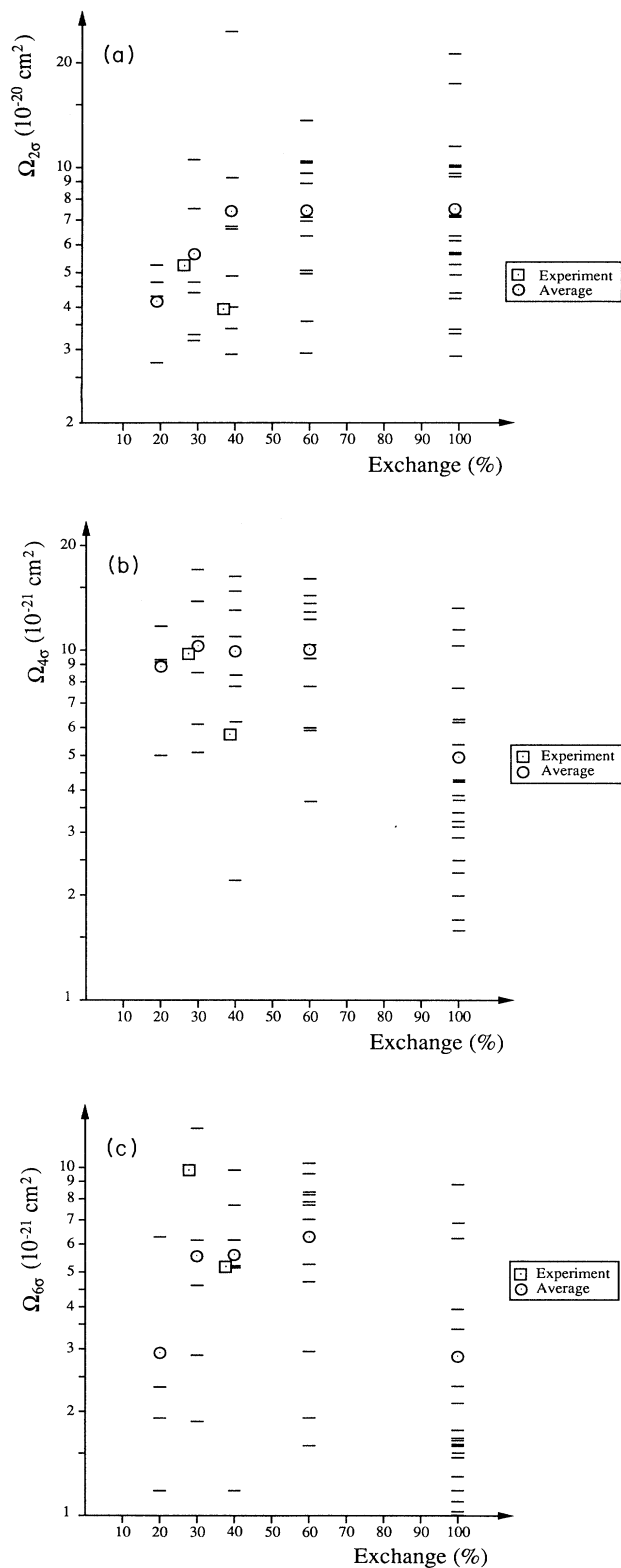
FIG. 4. Calculated $\Omega_{\lambda\sigma}$ parameters averaged over 500 time steps for the individual Nd^{3+} ions: (a) $\Omega_{2,\sigma}$, (B) $\Omega_{4,\sigma}$ and (c) $\Omega_{6,\sigma}$. The average value taken over all sites, and the experimental values at 27.5% and 38.5% are also included from Refs. 3 and 7.

TABLE IV. (a) Calculated σ-polarized JO intensity parameters averaged over all ions, and corresponding values for the 27.5% and 38.5% compositions (Refs. 3 and 7). (b) As (a), for the calculated π-polarized parameters and experimental values for the 38.5%, in units of 10^{-21} cm^2.

(a)			
% (Nd^{3+})	$\Omega_{2,\sigma}$	$\Omega_{4,\sigma}$	$\Omega_{6,\sigma}$
20	42(11)	8.9(2.9)	2.9(2.3)
30	56(28)	10.3(4.4)	5.5(3.7)
40	77(69)	9.9(5.0)	5.5(2.5)
60	74(34)	10.1(3.6)	6.3(2.9)
100	75(43)	4.9(3.2)	2.7(2.2)
27.5 (expt.)	51.9	9.73	9.71
38.5 (expt.)	39.6	5.62	5.09
(b)			
Exch. (%)	$\Omega_{2,\pi}$	$\Omega_{4,\pi}$	$\Omega_{6,\pi}$
20	42(10)	12(5)	4.7(5)
30	67(31)	16(9)	10(8)
40	81(68)	15(7)	9.5(5.0)
60	87(32)	17(7)	11(6)
100	83(43)	7.9(6.0)	4.3(4.0)
38.5 (expt.)	10.7	10.3	7.5

for the analysis is far too small (especially at low concentrations) to provide a statistically valid sample. A significantly larger simulation box and a larger number of time steps should be used. This is practically unrealistic for the time being. The present results should be seen rather as providing values typical of the real situation.

The effect of thermal motion of the Nd^{3+} ion environment on the Ω_λ parameters is plotted in Fig. 6 for one ion
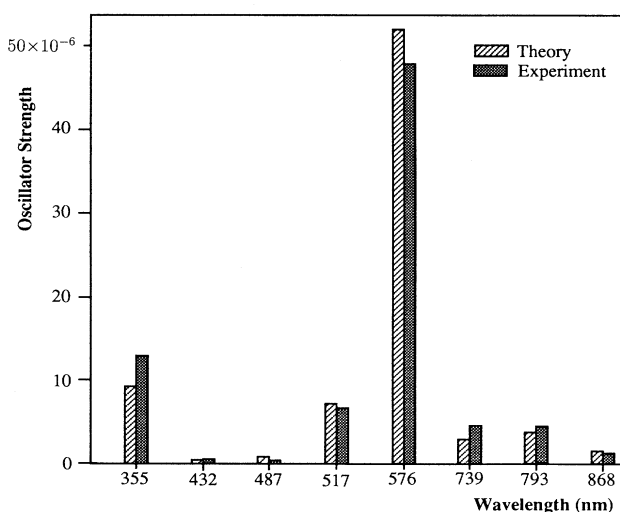

FIG. 5. Schematic comparison of experimental (27.5%) and theoretical (30%) oscillator strengths (σ polarization). The theoretical values are the averaged values over all sites, 500 MD time steps, and the transitions specified in Ref. 7.
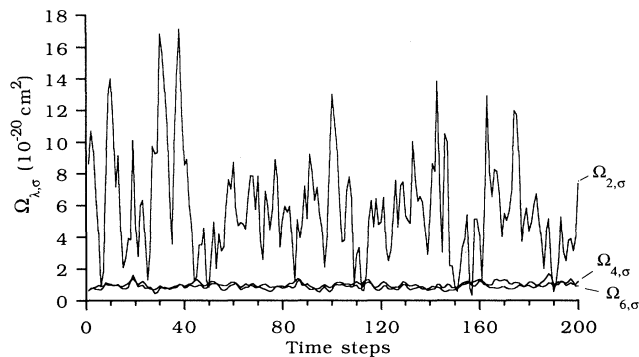
FIG. 6. Variation of the $\Omega_{\lambda,\sigma}$ parameters for one ion during 200 time steps of an MD simulation for the 40% composition at 300 K.

TABLE V. JO intensity parameters ($\Omega_{\lambda,\sigma}$) for the individual Nd^{3+} ions in the 60% composition. The values are averaged over 500 time steps, and expressed in units of 10^{-21} cm^2.

Ion No.	Site	$\Omega_{2,\sigma}$	$\Omega_{4,\sigma}$	$\Omega_{6,\sigma}$
1	mO	136	12.1	8.3
2	mO	96.1	9.4	4.7
3	mO	69.5	14	7.7
4	BR	70.4	10.5	8.2
5	mO	49.7	3.7	1.6
6	BR	35.7	7.8	7.1
7	BR	29.2	13.3	7.9
8	mO	103	6.1	5.3
9	mO	88.4	10.3	2.9
10	mO	102	5.9	1.8
11	BR	63.6	12.8	10.4
12	BR	50.1	15.7	9.6

for the 30% exchanged sample at 300 K during 200 time steps (0.4 ps). The plot confirms that Ω_2 is the sensitive parameter.[4,9] It further shows the necessity of using an average value for a succession of MD time steps. In an analysis of a β''-alumina structure, studies of this type are of extra importance because of the dynamics in the conduction planes and the nonstoichiometry. If, for example, a sodium ion moves between two sites, there will be a significant change in the crystal field experienced by the neighboring ions.

A particularly interesting feature of the experimental absorption spectra is the anomalously high value for the oscillator strength of the hypersensitive transition $^4I_{9/2} \rightarrow {}^4G_{5/2}$. It has been shown[9] that the Ω_2 parameter varies as the square of the electric field created by the ligands at the RE site and, in combination with a large value of the reduced matrix element $U^{(2)}$, this results in hypersensitivity. We see here that the highest Ω_2-parameter values are obtained when the ion is situated in a relatively high electric field. A typical example of this is the high value obtained for one of the ions in the 40% composition [see Fig. 4(a)]. The square of the electric field for this particular ion was roughly a factor ten larger than that for the other ions. This type of effect is unlikely to occur in low concentration samples, where sodium ions are more evenly distributed around the individual Nd^{3+} ions, leading to a lower, somewhat more "smeared out" electric field. In particular, the range of Ω_2 values is smaller for lower concentration samples. This, to some extent, compensates for the poor statistics for these concentrations, since the number of ions included in the calculations is smaller (cf. Fig. 4).

It emerges clearly from these calculations that, for disordered systems like β''-alumina, the concept of point symmetry in the context of JO theory loses much of its relevance. This implies that it is not possible to predict, on the basis of crystallographic point-symmetry considerations, how an ion in a BR or mO site will contribute to the spectrum. Theory requires that an ion at an mO site should not contribute to the spectra, since it is a center of inversion in the structure (leading to $A_{t,p}=0$ for t odd). We can note, however, that the *highest* Ω_2 parameters are actually obtained for ions at these mO sites in

the 60% case (see Table V). The ions in the disordered conduction planes break with the local average crystal symmetry. There is, on the other hand, at least a tendency for BR-site ions to actually yield higher Ω_6-parameter values than ions occupying mO sites, in accordance with the simple symmetry requirements. Clearly, nearest neighbors (the oxygens of the crystalline framework) are more important in determining the Ω_6 parameter, due to the R dependence of the crystal-field parameters [cf. earlier discussion and Fig. 3(b)].

D. Nd^{3+}-rich Na^+ β''-alumina

The $\Omega_{\lambda,\sigma}$-parameter values calculated here fall generally in the same range as the experimental values obtained for comparable concentrations (given in Fig. 4 of Ref. 3). A notable exception is the $\Omega_{2,\sigma}$ parameter for Nd^{3+}-rich Na^+ β''-alumina. This sample had a Nd^{3+} concentration of 1.7×10^{21} cm^{-3}, corresponding to 92% exchanged (a $Na^+:Nd^{3+}$ ratio of $\sim 1{:}4$). The corresponding $\Omega_{2,\sigma}$-parameter value was $\sim 1 \times 10^{-20}$ cm^2, while other experimental $\Omega_{2,\sigma}$ parameters lie in the range $3-6 \times 10^{-20}$ cm^2. Theoretical average values *all* lie in the region $4-7.5 \times 10^{-20}$ cm^2 (see Table IV). The reason for this discrepancy is somewhat obscure: No such variation was observed in recent experimental studies of Er^{3+}-doped Na^+ β''-alumina.[1] ESR and optical-absorption measurements indicates the possible formation of Nd^{3+} pairs at higher concentrations.[13] Such pairs would give rise to new levels at higher energies, and it was suggested that a combination of pairs and isolated Nd^{3+} ions could account for the differences in the optical spectra at higher concentrations. No discussion of what defines a "pair" was given, however. Since the presence of such pairs would also be expected to give rise to new absorption peaks at slightly different energies, these should naturally be included in the JO analysis. Experimental studies using high-resolution TEM have given evidence of superlattice formation amongst the Nd^{3+} ions of high-concentration Nd^{3+}-doped Na^+ β''-alumina.[20] This ordered structure was found to coexist with approximately equal quantities of a "disordered" structure, and was also

highly dependent on heat treatment after ion exchange. The effect of such ordering on the optical properties is unclear, and it would thus be relevant to perform optical-absorption experiments for samples with different thermal histories. The time scale of the annealing process (~ hours) makes it impossible to probe this ordering directly with the MD technique.

E. π-polarized spectra

The calculations of the π-polarized spectra can only be compared with experiments performed on the 38.5% composition [see Table 4(b)]. It is seen that agreement for the $\Omega_{2\pi}$ parameter is quite poor. It is a matter of some concern that crystal-field calculations give reasonable agreement for σ-polarized spectra, but not for the π-polarized case. Further studies of other compositions under well-controlled experimental conditions are needed before a more detailed analysis is meaningful.

F. Choice of radial integrals and energy denominators

As has been discussed by several authors,[3,8,21] a number of effects are not properly accounted for in the JO theory (ligand polarizability, shielding, penetration of the ligand wavefunction into the RE ion, etc.). Moreover, numerical uncertainties also arise as to the appropriate values for the radial integrals and energy denominators [see Eq. (4)]. Our present treatment retains the original formulation of the theory. We have examined the effect of using different radial integrals and energy denominators, however. Using the second set of values, given in Table III, we see that averaging Ω_λ parameters over 125 time steps of the 100% composition simulation causes $\Omega_{2,\sigma}$ to decrease from 70 to 36×10^{-21} cm^2, $\Omega_{4,\sigma}$ from 4.6 to 2.1×10^{-21} cm^2, and $\Omega_{6,\sigma}$ from 2.4 to 1.0×10^{-21} cm^2.

This clearly indicates that special care must be exercised in the calculation and measurement of these parameters.

VI. CONCLUSIONS

We see then that it is possible to achieve both a qualitative and quantitative understanding of the intensities of the absorption spectra of Nd^{3+}-doped Na^+ β''-alumina, using a simple point-charge model for calculating the crystal-field parameters. The criteria for this are (i) Proper account must be taken of the range of possible environments experienced by the Nd^{3+} ions, (ii) The thermal motion of the ions in the conduction plane must be included in the calculation, and (iii) A of a sufficiently large calculation sphere (or the Ewald summation method) must be used in the calculation of the $A_{t,p}$ parameters. This we have done by using a molecular-dynamics (MD) based Judd-Ofelt analysis as described in Ref. 9. A complete test of the crystal-field calculation and the structural model should also include treatment of the energy levels. This can be done in a similar manner.[22] We have seen that the complexity of the β''-alumina structure and limited computational capacity impose certain limitations on this work, e.g., size of simulation box, number of ions, number of time steps, size of calculation sphere. Other factors, such as choice of radial integrals and energy denominators, must also be considered in a more rigorous JO treatment.

ACKNOWLEDGMENTS

[1]H. Dai, Ph.D. thesis, University of California, Los Angeles, 1990.

[2]M. Jansen, A. J. Alfrey, O. M. Stafsudd, D. L. Yang, B. Dunn, and G. C. Farrington, Opt. Lett. **9**, 119 (1984).

[3]A. J. Alfrey, O. M. Stafsudd, B. Dunn, and D. L. Yang, J. Chem. Phys. **88**, 707 (1988).

[4]B. R. Judd, Phys. Rev. **127**, 750 (1962).

[5]G. S. Ofelt, J. Chem. Phys. **37**, 511 (1962).

[6]W. F. Krupke, Phys. Rev. **145**, 325 (1966).

[7]H. Dai and O. M. Stafsudd, J. Phys. Chem. Solids **52**, 367 (1991).

[8]M. C. Downer, G. W. Burdick, and D. K. Sardar, J. Chem. Phys. **89**, 1787 (1988).

[9]S. Edvardsson, M. Wolf, and J. O. Thomas, Phys. Rev. B **45**, 10 918 (1992).

[10]B. Dunn, G. F. Farrington, and J. O. Thomas, Mater. Res. Bull. **14**(9), 22 (1989).

[11]W. Carrillo-Cabrera, J. O. Thomas, and G. F. Farrington, Solid State Ionics **28-30**, 317 (1988).

[12]M. Wolf and J. O. Thomas, Acta Crystallogr. B **49**, 491 (1993).

[13]B. Dunn, D. L. Yang, and D. Vivien, J. Solid State Chem. **73**, 235 (1988).

[14]M. A. Zendejas and J. O. Thomas, Solid State Ionics **28-30**, 46 (1988).

[15]W. Smith and M. J. Gillian, J. Phys. Condens. Matter **4**, 3215 (1992).

[16]G. V. Lewis and C. R. A. Catlow, J. Phys. C **18**, 1149 (1985).

[17]J. R. Walker and C. R. A. Catlow, J. Phys. C **15**, 6151 (1982).

[18]K. L. Vander Sluis and L. J. Nugent, J. Chem. Phys. **60**, 1927 (1974).

[19]M. Faucher and P. Caro, J. Chem. Phys. **66**, 1273 (1977).

[20]P. Davies, A. Petford, and M. O'Keefe, Solid State Ionics **18-19**, 624 (1986).

[21]D. J. Newman, Adv. Phys. **20**, 197 (1971).

[22]M. J. Weber and S. A. Brawer, J. Non-Cryst. Solids **52**, 321 (1982).